THE CROP JOURNAL 8 (2020) 182–193

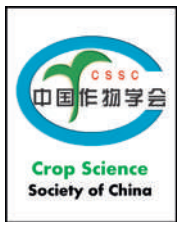

Available online at www.sciencedirect.com

ScienceDirect

Genetic analysis of the seed dehydration process in maize based on a logistic model

Shuangyi Yin[a], *Jun Liu*[a], *Tiantian Yang*[a], *Pengcheng Li*[a], *Yang Xu*[a], *Huimin Fang*[a], *Shuhui Xu*[a], *Jie Wei*[a], *Lin Xue*[b], *Derong Hao*[b], *Zefeng Yang*[a,*], *Chenwu Xu*[a,*]

[a]*Jiangsu Provincial Key Laboratory of Crop Genetics and Physiology, Co-Innovation Center for Modern Production Technology of Grain Crops, Key Laboratory of Plant Functional Genomics of Ministry of Education, Yangzhou University, Yangzhou 225009, Jiangsu, China*
[b]*Jiangsu Yanjiang Institute of Agricultural Sciences, Nantong 226541, Jiangsu, China*

ARTICLE INFO

Article history:
Received 4 April 2019
Received in revised form 28 May 2019
Accepted 27 July 2019
Available online 20 October 2019

Keywords:
Maize
Dehydration
Logistic model
Characteristic parameter
QTL

ABSTRACT

Seed moisture at harvest is a critical trait affecting maize quality and mechanized production, and is directly determined by the dehydration process after physiological maturity. However, the dynamic nature of seed dehydration leads to inaccurate evaluation of the dehydration process by conventional determination methods. Seed dry weight and fresh weight were recorded at 14 time points after pollination in a recombinant inbred line (RIL) population derived from two inbred lines with contrasting seed dehydration dynamics. The dehydration curves of RILs were determined by fitting trajectories of dry weight accumulation and dry weight/fresh weight ratio change based on a logistic model, allowing the estimation of eight characteristic parameters that can be used to describe dehydration features. Quantitative trait locus (QTL) mapping, taking these parameters as traits, was performed using multiple methods. Single-trait QTL mapping revealed 76 QTL associated with dehydration characteristic parameters, of which the phenotypic variation explained (PVE) was 1.03% to 15.24%. Multiple-environment QTL analysis revealed 21 related QTL with PVE ranging from 4.23% to 11.83%. Multiple-trait QTL analysis revealed 58 QTL, including 51 pleiotropic QTL. Combining these mapping results revealed 12 co-located QTL and the dehydration process of RILs was divided into three patterns with clear differences in dehydration features. These results not only deepen general understanding of the genetic characteristics of seed dehydration but also suggest that this approach can efficiently identify associated genetic loci in maize.

* *Corresponding authors.*
E-mail addresses: zfyang@yzu.edu.cn, (Z. Yang), cwxu@yzu.edu.cn. (C. Xu).
Peer review under responsibility of Crop Science Society of China and Institute of Crop Science, CAAS.

https://doi.org/10.1016/j.cj.2019.06.0112214-5141

1. Introduction

Seed moisture at harvest is critical for maize quality and mechanized production. In some areas with high latitude or altitude, rainfall is greater and daylight is shorter, with a rapid decline in temperature after autumn. At low temperature and in a wet and climate with short days, seed moisture is too high to allow rapid dehydration, leading to mildewed grain with reduced commercial quality [1]. Even with artificial drying, drying time is prolonged by high grain moisture content, incurring labor and financial costs. High moisture also leads readily to seed breakage during mechanized harvesting, reducing mechanized production efficiency. For these reasons, breeding of maize varieties with low moisture at harvest is an important goal for breeders.

The change in seed moisture comprises two distinct phases [2]. The first phase spans the time from the successful pollination and initiation of seed development to seed physiological maturity. During this phase, water loss in the seed is due primarily to dry matter accumulation in the filling process. The second phase spans the time from physiological maturity to grain harvest and is defined as the seed dehydration process [2,3]. In this process, seed moisture at physiological maturity, length of dehydration time, and dehydration rate jointly determine seed moisture at harvest. Seed dehydration is a continuous and dynamic process in which the moisture at each time point is affected by that at the previous moment.

The dynamic nature of the dehydration process poses a challenge to QTL mapping because, at individual developmental stages or time points, different sets of genes are involved. However, because of the importance of seed moisture in production, researchers have studied the seed dehydration process using diverse approaches. Most have treated seed dehydration as a linear-change process and determined the physiological maturity of maize from black-layer formation and milk-line disappearance [4,5]. This approach is too imprecise for quantitative analysis. An improved method [6,7] converts seed dry weight to 100-seed weight at 14% moisture content and defines physiological maturity as occurring at the maximum value of this measure. However, the harvest time, or time to reach a stable moisture content, have been treated as identical for all genotypes. In fact, different genotypes are likely to have different dehydration periods, especially in separate populations [8]. Furthermore, these approaches have focused only on average dehydration rate and failed to capture other dehydration features affecting final moisture, such as initial dehydration rate and dehydration duration.

A better strategy for studying such a time-dependent trait is to fit a curve to the phenotypic values across the entire dynamic process and analyze the fitted parameters of the change trajectory using quantitative genetic approaches. A typical example is the description of seed filling using a logistic function with a few fitted parameters [9]. Replacing phenotypic measurements at multiple time points with a few parameters with biological relevance revealed the genetic architecture associated with seed filling, indicating that this strategy is feasible and reliable. Concretely, the author defined the filling characteristic parameter t_3 as the attainment time of maximum grain dry weight, a definition consistent with that of physiological maturity [10]. This above information provides clues and inspiration for the study of seed dehydration.

The objectives of this study were to define the seed dehydration process based on a logistic model, to estimate several parameters that meaningfully describe dehydration features, and to identify QTL affecting these parameters using several methods. We wished to show that the strategy used in this study is suitable for analysis of the dynamic dehydration process and to deepen general understanding of the genetic characteristics of seed dehydration.

2. Materials and methods

2.1. Plant materials, field experiments, and phenotyping

A RIL population of 208 lines was derived from the cross of the parental genotypes DH1M and T877, which differed significantly in their dehydration features. DH1M has a long seed dehydration duration and low final moisture levels, whereas T877 has a much shorter seed dehydration duration and produces seeds with higher final moisture levels. The experiments were conducted at three geographically different locations in China: Nantong (31°55′N, 121°37′E) in 2015, Yangzhou (32°22′N, 119°16′E) in 2016, and Sanya (18°23′N, 109°44′E) in 2017. For each RIL, 78 plants were grown in a plot consisting of six rows, with a row length of 3.0 m, a distance between rows of 0.5 m, and 13 plants per row. The pollination dates were recorded for individual RILs to determine the sampling time. Seeds were sampled at 10, 15, 20, 25, 30, 35, 40, 43, 46, 49, 52, 55, 58, and 61 days after pollination (DAP). At each time point, two ears with synchronous developmental processes were selected. Fifty seeds in the middle of each ear were removed and their fresh weights were recorded. The seeds were then dried at 70–80 °C to constant weight after undergoing fixation at 105 °C for 1 h and their dry weight was recorded.

2.2. Dehydration curve determination and parameter estimation

The relationship between seed dry weight w and number of days after pollination t may be described by a logistic function [11]:

$$w = \frac{k}{1 + ae^{-bt}} \quad (1)$$

where, k, a, and b are fitted parameters; k estimates the final or upper limit of seed dry weight, b estimates the filling rate, and a is associated with both the rate and duration of seed filling.

Seed moisture at each time point may be calculated using the formula (1 – dry weight/fresh weight) × 100%, where the dry weight/fresh weight ratio increases with the accumulation of dry matter until it finally stabilizes, and follows a typical sigmoid curve that can also be fitted using

a logistic function [11]. Thus, using the relationship between moisture and dry weight/fresh weight ratio, seed moisture m is calculated as

$$m = 1 - \frac{k_{dfr}}{1 + a_{dfr} e^{-b_{dfr} t}} \quad (2)$$

where k_{dfr} estimates the final or upper limit of the dry weight/fresh weight ratio, b_{dfr} is the relative change rate of the dry weight/fresh weight ratio, and a_{dfr} is associated with both the change rate and duration of seed dehydration. The seed final moisture was recorded as m_{fin} and can be obtained using k_{dfr} as follows:

$$m_{fin} = 1 - k_{dfr}$$

Theoretically, seed dry weight will approach the asymptotic maximum k. Under the assumption that the seed completes physiological maturation and enters dehydration when $w = 0.99\ k$ [9], the dehydration initial time is calculated by substituting $0.99\ k$ for w in Eq. (1). Similarly, the parameter m_{fin} is also a theoretical asymptotic value. It may be assumed that when the change in seed moisture is equal to 99% of the total change in moisture, the seed moisture will no longer change and the dehydration process is complete. The dehydration initial time (t_{ini}) and dehydration final time (t_{fin}) may be accordingly calculated as follows:

$$t_{ini} = \frac{\ln(99a)}{b} \text{ and } t_{fin} = \frac{\ln(99a_{dfr} + 100)}{b_{fdr}}$$

Using t_{ini}, t_{fin}, and Eqs. (1) and (2), the seed dehydration curve may be drawn (Fig. 1). Based on t_{ini} and t_{fin}, the seed dehydration duration (t_{deh}) can be calculated as follows:

$$t_{deh} = \frac{\ln(99a_{dfr} + 100)}{b_{fdr}} - \frac{\ln(99a)}{b}.$$

Substituting t_{ini} for t in Eq. (2), yields the dehydration initial moisture (m_{ini}) using the equation

$$m_{ini} = 1 - \frac{k_{dfr}}{1 + a_{dfr}(99a)^{-\frac{b_{dfr}}{b}}}$$

Subtracting m_{fin} from m_{ini} yields the change of seed moisture during the dehydration process (m_{deh}), using the equation

$$m_{deh} = \frac{k_{dfr} a_{dfr}(99a)^{-\frac{b_{dfr}}{b}}}{1 + a_{dfr}(99a)^{-\frac{b_{dfr}}{b}}}$$

The average dehydration rate (v_{deh}) from m_{deh} and t_{deh} follows:

$$v_{deh} = \frac{k_{dfr} a_{dfr} b_{dfr} b(99a)^{-\frac{b_{dfr}}{b}}}{\left[1 + a_{dfr}(99a)^{-\frac{b_{dfr}}{b}}\right][b\ \ln(99a_{dfr} + 100) - b_{dfr}\ \ln(99a)]}$$

The instantaneous rate (v) of seed dehydration at time t may be expressed as the first derivative, with respect to t, of the expression in Eq. (1).

$$v = -\frac{k_{dfr} a_{dfr} b_{dfr} e^{-b_{dfr} t}}{(1 + a_{dfr} e^{-b_{dfr} t})^2} \quad (3)$$

Based on this equation, the initial dehydration rate (v_{ini}) may be obtained by substitution of t_{ini} for t in Eq. (3), as follows:

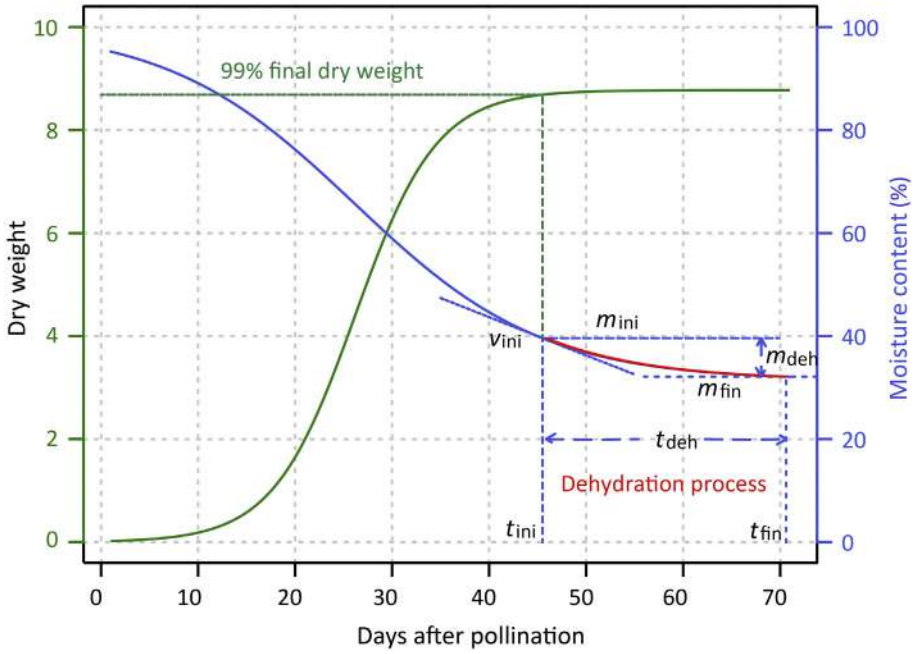

Fig. 1 – A diagrammatic representation of the dry weight accumulation curve (green), dry weight/fresh weight ratio curve (blue), and seed dehydration curve (red). Several seed dehydration characteristic parameters are included. v_{ini} is the initial dehydration rate, t_{ini} is the dehydration initial time, m_{ini} is the dehydration initial moisture, t_{deh} is the dehydration duration, m_{deh} is the change in moisture during the dehydration process, m_{fin} is the final moisture, and t_{fin} is the final dehydration time.

$$v_{ini} = \frac{k_{dfr} a_{dfr} b_{dfr} (99a)^{-\frac{b_{dfr}}{b}}}{\left[1 + a_{dfr} (99a)^{-\frac{b_{dfr}}{b}}\right]^2}$$

Thus, eight characteristic parameters describing the seed dehydration process may be estimated. The symbols of these parameters, together with their biological definitions, are listed in Table 1. Parameters k, a, b, k_{dfr}, a_{dfr}, and b_{dfr} may be estimated using a nonlinear least-quares approach implemented in R [12].

2.3. Statistical analysis of the parameters

Descriptive statistics of the parameters were calculated with R. Broad-sense heritability (H^2) across multiple environments was estimated following Knapp [13], where δ_g^2 is genetic variance, δ^2 is error variance, and e is number of environments. Pearson correlation coefficients among characteristic parameters were calculated using the *agricolae* software package [14,15].

2.4. Genotyping and bin-map construction

DNA of RILs and the two parents were extracted from young, healthy leaves. The Illumina MaizeSNP50 BeadChip [16] containing over 56,110 single-nucleotide polymorphisms (SNPs) evenly distributed throughout the genome was used for genotyping. Based on chi-square tests, SNPs with a segregation distortion test significance of $P < 0.001$ or containing abnormal bases were filtered out. A genetic linkage map was constructed using a sliding-window approach [17]. The code used for linkage map construction may be found in the supplementary data. The markers with same segregation pattern were converted into bin data. Each bin is considered a new marker for linkage mapping. The order of markers was then checked using the *ripple* function in the *R/qtl* package [18]. Genetic distances between bin markers were calculated using the Kosambi function [19].

2.5. QTL analysis

QTL analysis for seed dehydration characteristic parameters was performed by several methods. Single-trait QTL mapping was performed using composite interval mapping (CIM), with a window size of 10 cM and a step size of 1 cM in *R/qtl* [18]. Multiple-environment QTL mapping was performed using inclusive composite interval mapping (ICIM) in IciMapping [20–22]. QTL by environment interaction scanning was implemented based on default parameters. Multiple-trait QTL mapping was performed by multiple-trait composite interval mapping (Mt-CIM) with default parameters in Windows QTL Cartographer 2.5 [23]. To avoid the loss of QTL with small effects, LOD thresholds were empirically set as respectively 2.5, 3.0, and 3.5 for single-trait, multiple-environment, and multiple-trait QTL mapping. The total genetic variance explained by all QTL for each characteristic parameter was estimated by multiple interval mapping (MIM) in Windows QTL Cartographer 2.5 [24].

Table 1 – Characteristic parameters associated with seed dehydration.

Parameter symbol	Biological significance
t_{ini}	Dehydration initial time (DAP)
m_{ini}	Dehydration initial moisture
v_{ini}	Initial dehydration rate
t_{deh}	Dehydration duration (days)
m_{deh}	Moisture change during dehydration process
v_{deh}	Average dehydration rate
m_{fin}	Final moisture
t_{fin}	Dehydration final time (DAP)

2.6. Co-located QTL identification and dehydration pattern division

Using the results of QTL scanning, co-located QTL were identified with the *qtlhot* package [25,26]. Based on these identified co-located QTL, seed dehydration processes were divided into several patterns using the *hclust* function. Differences in dehydration characteristic parameters among patterns were tested by analysis of variance (ANOVA).

3. Results

3.1. Seed dehydration trajectories and related characteristic parameters

To obtain the dehydration trajectories of each inbred line, seed filling curves and moisture curves of 208 RILs were fitted across three different environments. The mean coefficients of determination (R^2) of filling curves in Nantong in 2015, Yangzhou in 2016, and Sanya in 2017 were 0.95, 0.95, and 0.97, respectively. The mean R^2 values of moisture curves were 0.98, 0.95, and 0.98, respectively. These results indicate that the logistic function provided a good fit for the changes in dry weight and moisture. Seed dehydration trajectories were drawn based on change processes of seed filling and moisture (Fig. 2-A). The dehydration processes of the 208 RILs showed marked differences across the three environments. For parents, the dehydration duration of DH1M was longer than that of T877 and the final moisture of T877 was greater than that of DH1M in all three environments. The eight characteristic parameters associated with the dehydration process are described in Table 2. The observation that the minimum value of t_{deh} is negative indicates that seed moisture stabilized before the filling process stopped. At that moment, the characteristic parameters describing the dehydration rate and changes of moisture were very small and approached zero. All characteristic parameters among the RILs showed wide variation, with coefficients of variation ranging from 12.7% to 234.7%. The H^2 of these characteristic parameters ranged from 53.7% to 82.6%, where m_{fin} had the smallest and m_{deh} the largest H^2. Thus, the segregating population showed high genetic variation for seed dehydration dynamics.

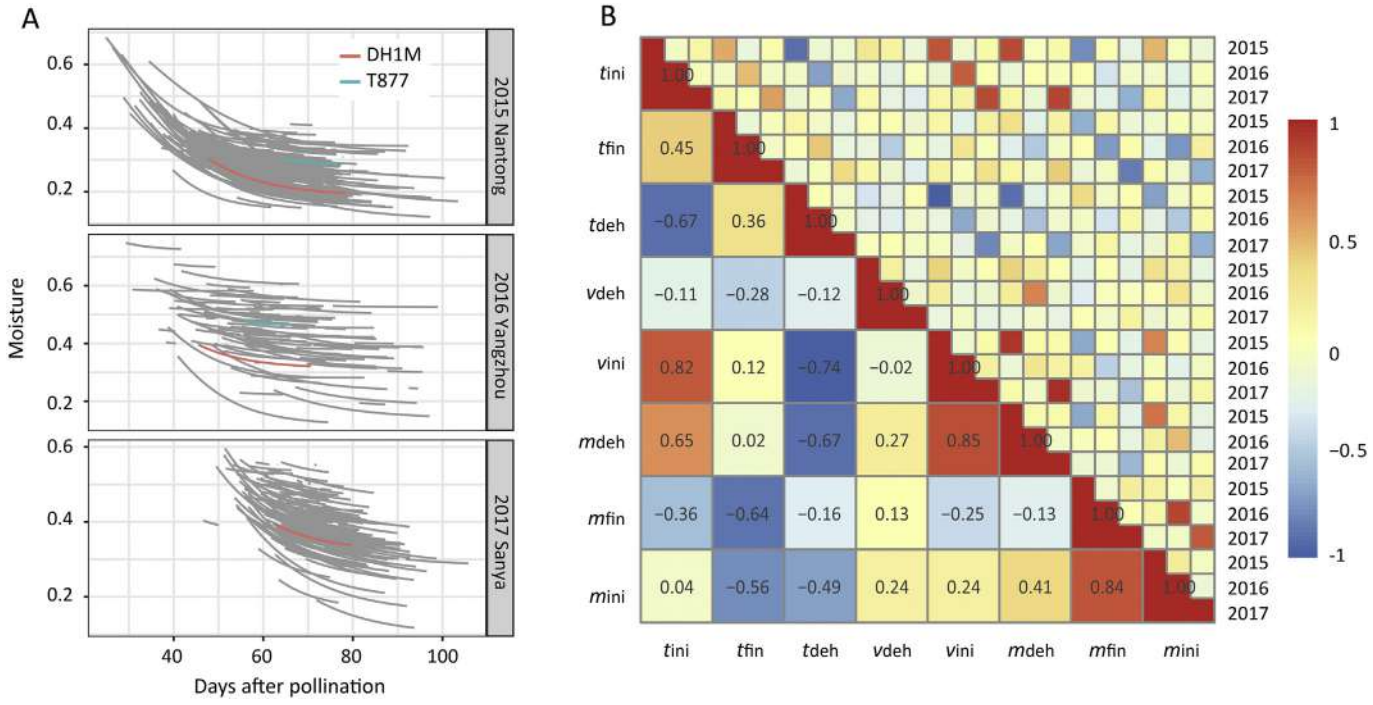

Fig. 2 – Seed dehydration curves of two parents and RILs (gray) in three environments, and correlations among dehydration characteristic parameters. A) Red curves represent dehydration processes of DH1M and blue curves represent dehydration processes of T877. The dehydration curves of the RILs show wide variation in three environments. B) The lower left diagonal displays the correlations among characteristic parameters based on the three environments. The upper right diagonal displays correlations among characteristic parameters based on a single environment. Red indicates positive and blue indicates negative correlation. The darker the color, the stronger is the correlation.

3.2. *Correlations between characteristic parameters associated with dehydration*

Pearson correlation coefficients between characteristic parameters are illustrated in Fig. 2-B. A high positive correlation was found between m_{ini} and m_{fin}. Interestingly, there was a negative correlation between m_{fin} and t_{fin} that was stronger than the correlations between m_{fin} and other parameters associated with dehydration time. Also, m_{deh} showed high positive correlations with t_{ini} and v_{ini}, indicating that a higher initial dehydration rate was associated with a larger change in moisture content. Moreover, the dehydration duration would be shorter owing to the negative correlation between t_{ini} and t_{deh}. As evident from the low correlations among the three environments for each parameter, these characteristic parameters may be affected by genotype–environment interaction.

3.3. *Construction of the genetic linkage map*

The genetic linkage map with 3227 bin markers is described in Table S1 and Fig. 3. The map covered 2450 cM, with a mean interval length of 0.76 cM. Chromosome length varied from 373.06 cM (chromosome 1) to 102.29 cM (chromosome 2). The number of markers per chromosome varied from 503 to 111, with chromosome 1 containing the most markers (503) and chromosome 2 the fewest (111). The maximum marker interval per chromosome ranged from 5.65 cM (chromosome 5) to 25.39 cM (chromosome 7). Chromosome 5 showed the largest marker density, with a mean interval length of 0.64 cM. Chromosome 7 showed the smallest marker density, with a mean interval length of 0.91 cM.

3.4. *QTL analysis*

3.4.1. *QTL for a single characteristic parameter in a single environment*

All QTL identified by single-trait QTL mapping in any of the three environments are summarized in Table S2. The 76 QTL included 31 in Nantong in 2015, 25 in Yangzhou in 2016, and 20 in Sanya in 2017. The logarithm of odds (LOD) curves are shown in Fig. 4-A, where it is evident that the same characteristic parameters showed different peaks in different environments. These QTL were potentially affected by environment. Some QTL for the same characteristic parameters were repeatedly detected in multiple environments, such as a QTL for t_{ini} on chromosome 7 and one for v_{ini} on chromosome 8. Some QTL were repeatedly detected for different characteristic parameters, suggesting the action of pleiotropic loci. In Nantong in 2015, the total phenotypic variation explained (PVE) for each characteristic parameter ranged from 9.04% to 30.19%. In Yangzhou in 2016, m_{ini} showed the highest total PVE (35.90%) and t_{fin} the lowest (1.23%). In Sanya in 2017, m_{fin} showed the highest total PVE (30.27%) and v_{deh} showed the lowest (2.21%). Across the three environments, the proportion of phenotype variation explained by a single QTL ranged from

Table 2 – Descriptive statistics for eight characteristic parameters associated with dehydration process.

Characteristic parameters	Environment	DH1M	T877	RIL					
				Mean	Standard deviation	Maximum	Minimum	Coefficient of variation (%)	Heritability (%)
t_{deh}	2015 Nantong	30.520	12.190	22.043	14.004	57.740	−13.920	63.5	76.6
	2016 Yangzhou	25.100	9.370	7.890	14.692	39.180	−23.570	186.2	
	2017 Sanya	16.810	0.430	11.661	9.632	35.950	−15.790	82.6	
t_{fin}	2015 Nantong	78.450	76.841	72.842	9.160	103.515	42.306	12.6	72.7
	2016 Yangzhou	70.610	65.697	66.452	13.783	97.116	30.806	20.7	
	2017 Sanya	79.677	78.044	78.241	8.558	98.715	50.078	10.9	
t_{ini}	2015 Nantong	47.934	64.647	50.862	12.248	92.413	24.906	24.1	77.9
	2016 Yangzhou	45.508	56.323	58.947	14.513	99.030	29.357	24.6	
	2017 Sanya	62.864	77.613	66.695	8.465	105.787	46.610	12.7	
v_{deh}	2015 Nantong	0.004	0.002	0.004	0.003	0.041	0.000	89.0	78.1
	2016 Yangzhou	0.002	0.009	0.007	0.016	0.092	0.000	234.7	
	2017 Sanya	0.002	0.021	0.004	0.008	0.073	0.000	212.5	
v_{ini}	2015 Nantong	0.009	0.002	0.008	0.006	0.024	0.000	73.1	79.6
	2016 Yangzhou	0.007	0.002	0.003	0.003	0.019	0.000	118.5	
	2017 Sanya	0.003	0.001	0.003	0.002	0.009	0.000	69.6	
m_{deh}	2015 Nantong	0.115	0.022	0.099	0.092	0.447	0.001	92.5	82.6
	2016 Yangzhou	0.049	0.084	0.042	0.061	0.338	0.000	146.4	
	2017 Sanya	0.036	0.009	0.030	0.023	0.129	0.001	78.4	
m_{fin}	2015 Nantong	0.188	0.280	0.258	0.064	0.403	0.113	24.9	53.7
	2016 Yangzhou	0.314	0.459	0.429	0.103	0.725	0.118	24.1	
	2017 Sanya	0.160	0.159	0.183	0.041	0.272	0.049	22.3	
m_{ini}	2015 Nantong	0.302	0.302	0.357	0.078	0.685	0.182	21.9	65.3
	2016 Yangzhou	0.363	0.543	0.471	0.116	0.775	0.181	24.6	
	2017 Sanya	0.196	0.168	0.213	0.035	0.298	0.123	16.4	

1.03% to 15.24% (Fig. 4-B). For all parameters, the explained phenotype variation of most QTL was <10.00% and fewer loci made larger phenotypic contributions. Both parents contributed favorable alleles at various loci. T877 provided increasing QTL alleles for t_{ini}, m_{deh}, and m_{fin}, whereas DH1M provided increasing QTL alleles associated with t_{deh}, t_{fin}, and v_{deh} (Fig. 4-C). This observation is consistent with the observed phenotypic differences between the two parents.

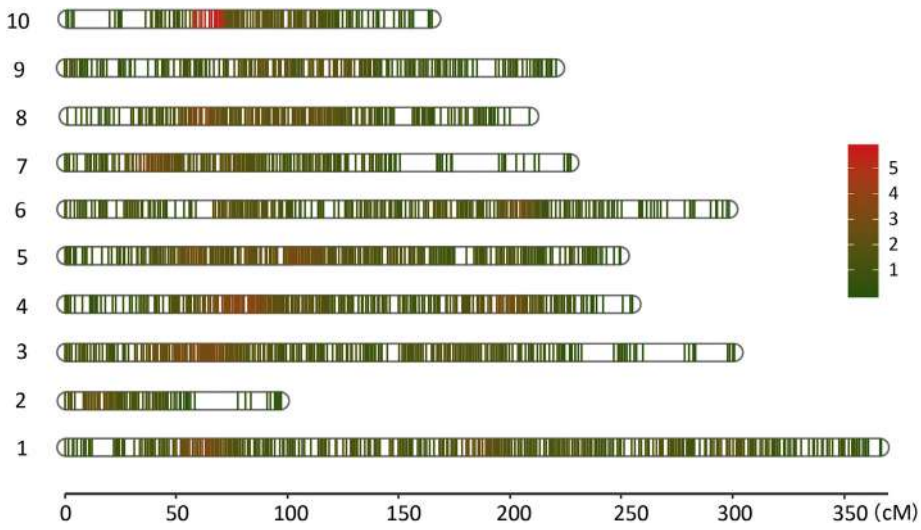

Fig. 3 – Distribution of markers in the linkage map. Colors indicate numbers of markers per cM.

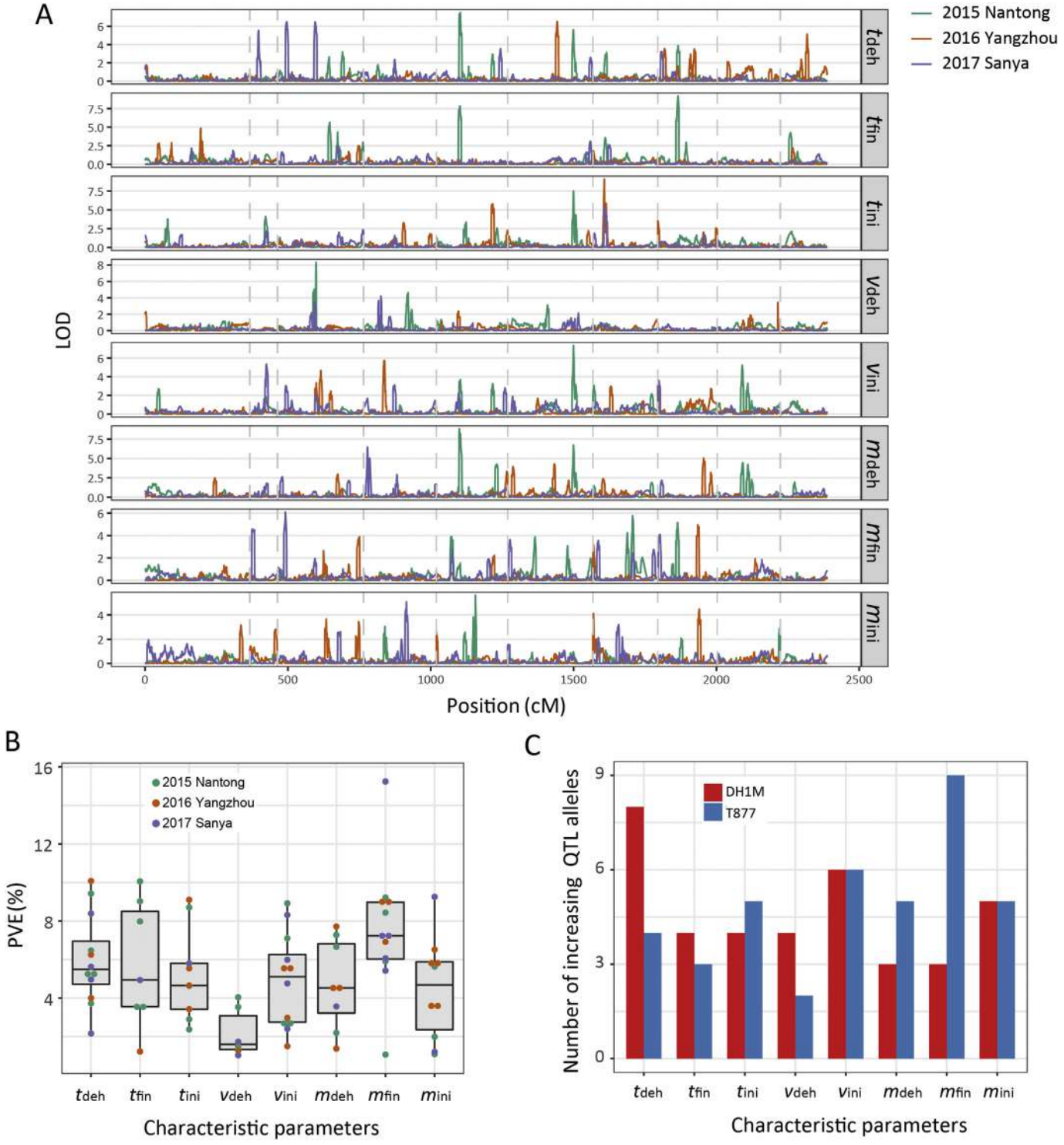

Fig. 4 – Single-trait QTL mapping of eight characteristic parameters. A) LOD curves of characteristic parameters in different environmental conditions. B) PVE distribution of the corresponding QTL for each characteristic parameter. Different colors represent different environments. C) The number of increasing QTL alleles for different parameters contributed by each parent. Blue bars indicate the numbers of increasing QTL alleles contributed by T877 and red bars indicate the numbers of increasing QTL alleles contributed by DH1M.

3.4.2. Multiple-environment QTL detection

The LOD profiles of characteristic parameters based on multiple-environment QTL analysis are shown in Fig. 5-A. The 21 QTL identified across the three environments included one for t_{deh}, four for t_{fin}, four for t_{ini}, two for v_{ini}, one for m_{deh}, seven for m_{fin}, and two for m_{ini} (Table S3). The mean PVE for

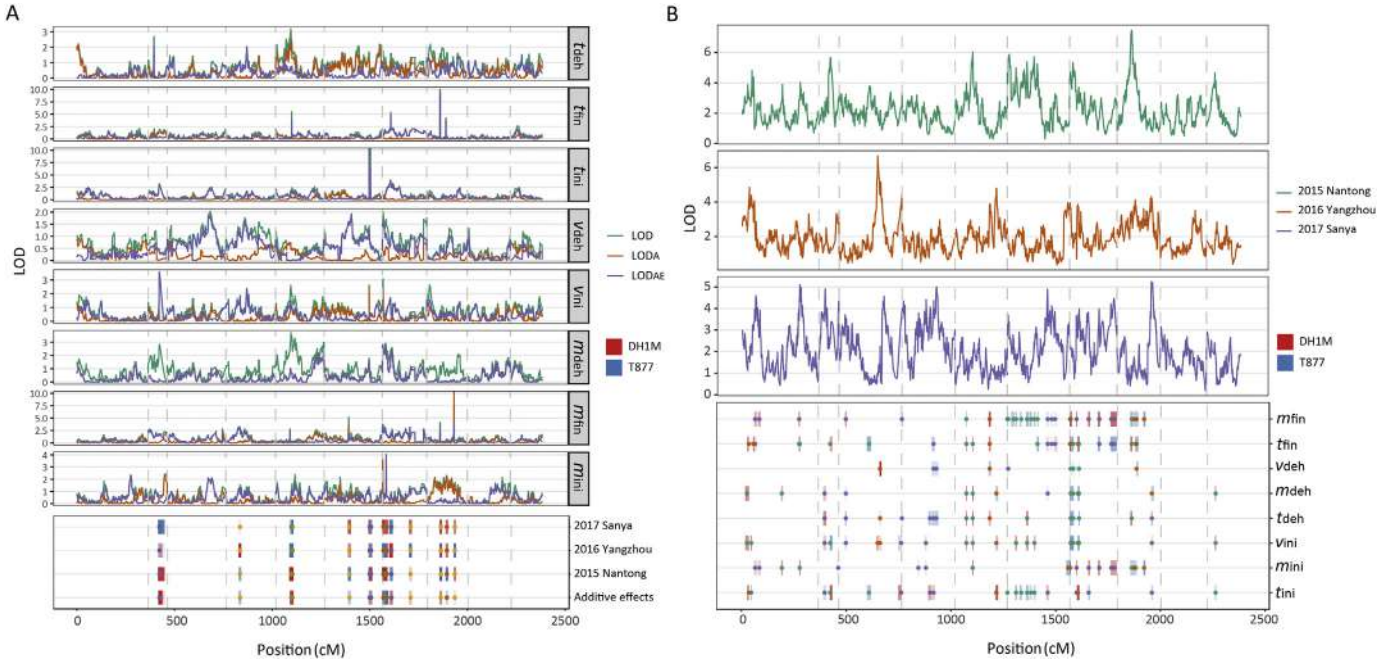

Fig. 5 – Profile plots for multiple-environment QTL mapping and multiple-trait QTL mapping. A) The LOD, LOD_A, and LOD_{AE} are the LOD scores for detecting QTL with both mean and environmental interaction effects, QTL with only mean effects, and QTL with only environmental interaction effects, respectively. Blue square means that the T877 allele had a positive effect and red square means that the DH1M allele had a positive effect. The darker the color, the larger is the effect value. B) The top section shows LOD curves of joint analysis in three environments. The bottom section shows heat maps along the genome for each characteristic parameter, where blue square means that the T877 allele had a positive effect and red square means that the DH1M allele had a positive effect. The darker the color, the larger is the effect value.

individual QTL ranged from 4.23% to 11.83%. The total PVE for each characteristic parameter ranged from 4.23% to 44.87%. Although QTL-by-environment interaction was detected in some regions, some QTL with a large LOD_A (LOD scores for QTL with only mean effects) and small LOD_{AE} (LOD scores for QTL with only environmental interaction effects) were relatively stable in different environments. In contrast, some QTL with small LOD_A and large LOD_{AE} showed strong QTL–environment interaction. A QTL for t_{ini} with a very large LOD was detected at 229.7 cM on chromosome 6 with a mean additive effect of 2.488, indicating that the allele from the parent T877 at this locus would delay initial dehydration time by 2.488 days based on the population mean. The PVEs of most QTL showed large environmental interaction, and the interactive effects of some QTL were larger than the additive effects. This result indicates that QTL–environment interaction was an important factor controlling these characteristic parameters and that dehydration features were strongly influenced by environments.

3.4.3. *Multiple-trait QTL analysis*

The results of multiple-trait analysis in each environment are shown in Fig. 5-B and Table S4. In Nantong during 2015, 22 QTL were detected, with 21 QTL being pleiotropic. For the eight characteristic parameters, the total PVE ranged from 11.23% to 59.95%. In Yangzhou during 2016, 13 QTL were detected, including nine pleiotropic QTL. The total PVE of these QTL for each characteristic parameter ranged from 4.78% to 24.64%. In Sanya during 2017, 23 QTL were detected, of which 21 QTL were pleiotropic. In total, 6.40%–38.69% of the phenotypic variance for each characteristic parameter was explained by these QTL. Thus, a total of 58 QTL were identified for dehydration characteristic parameters, of which 51 showed pleiotropic effects. Most pleiotropic QTL showed antagonistic pleiotropic effects and a few showed synergistic pleiotropic effects. Thirteen QTL were identified on chromosome 6, the largest number on a single chromosome. On chromosome 10, only one QTL was detected, and it controlled m_{deh}, v_{ini}, and t_{ini}. No QTL for seed dehydration were found on chromosome 9. Among the eight dehydration characteristic parameters, m_{fin} was controlled by the most QTL (31) and v_{deh} by the fewest (9). t_{ini}, m_{ini}, v_{ini}, t_{deh}, m_{deh}, and t_{fin} were controlled by 21, 19, 21, 16, 14, and 26 QTL, respectively. Of the pleiotropic QTL, most controlled two or three characteristic parameters. Five controlled four characteristic parameters. Only one QTL, located at 3.88 cM on chromosome 7, controlled six characteristic parameters. The pleiotropies of these QTL were consistent with correlations among the characteristic parameters. As an example, three QTL located at 140.8, 197.4, and 213.0 cM on chromosome 7 showed antagonistic pleiotropy between m_{ini} and t_{fin}, a finding consistent with the negative correlation between m_{ini} and t_{fin}.

3.5. *Co-located QTL and dehydration pattern*

QTL mapping based on multiple methods identified abundant loci associated with dehydration features. Overall,

characteristic parameters associated with seed dehydration were regulated by some major loci and some loci with environmental interactions or pleiotropic effects. However, stable and reliable QTL are most desirable for genetic improvement. Based on the results of QTL mapping, a total of 12 co-located QTL were identified across the genome (Fig. 6, Table S5). Chromosomes 2, 5, and 8 had one co-located QTL each. Chromosomes 3, 4, and 6 had two co-located QTL each. Three co-located QTL were identified on chromosome 7. The seed dehydration processes of RILs were divided into three patterns according to the 12 co-located QTL (Fig. 7-A). The seed dehydration processes under three patterns displayed obvious differences. The average dehydration curve of each environment was described by different patterns (purple dashed lines). The differences in dehydration features between patterns showed a consistent and regular pattern. To eliminate the influence of the environment, average dehydration curves based on the three environments under different patterns (blue solid lines) were drawn. The overall average dehydration process under pattern 1 showed a lagging initial dehydration time, low average dehydration rate, lagging final dehydration time, and low final moisture. The overall average dehydration process under pattern 2 showed an early initial dehydration time, high initial dehydration rate, long dehydration duration, large moisture change, high average dehydration rate, early final dehydration time, and high final moisture. The overall average dehydration process under pattern 3 showed a small initial dehydration rate and small moisture change. The differences of characteristic parameters associated with seed dehydration between different patterns were inspected (Fig. 7-B). All parameters showed clear differences among different patterns, except for t_{deh}. This finding indicates that the 12 co-located loci were reliable and could effectively divide the seed dehydration process.

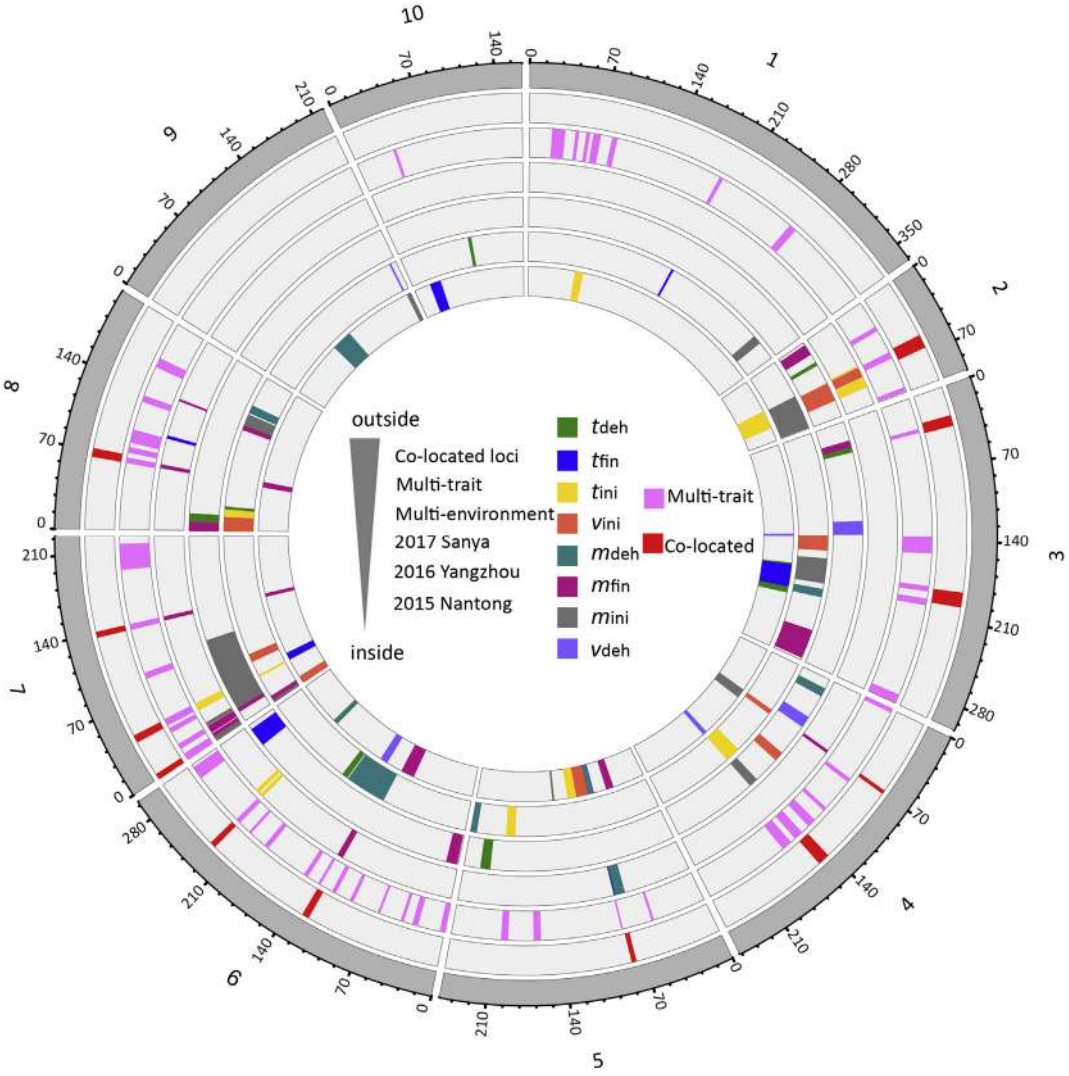

Fig. 6 – Distribution along the genome of QTL detected by multiple mapping methods. From the center to the outside of the image are QTL detected by single-trait mapping, QTL detected by multiple-environment mapping, QTL detected by multiple-trait mapping, and co-located QTL. Different colors represent QTL from different characteristic parameters and mapping methods.

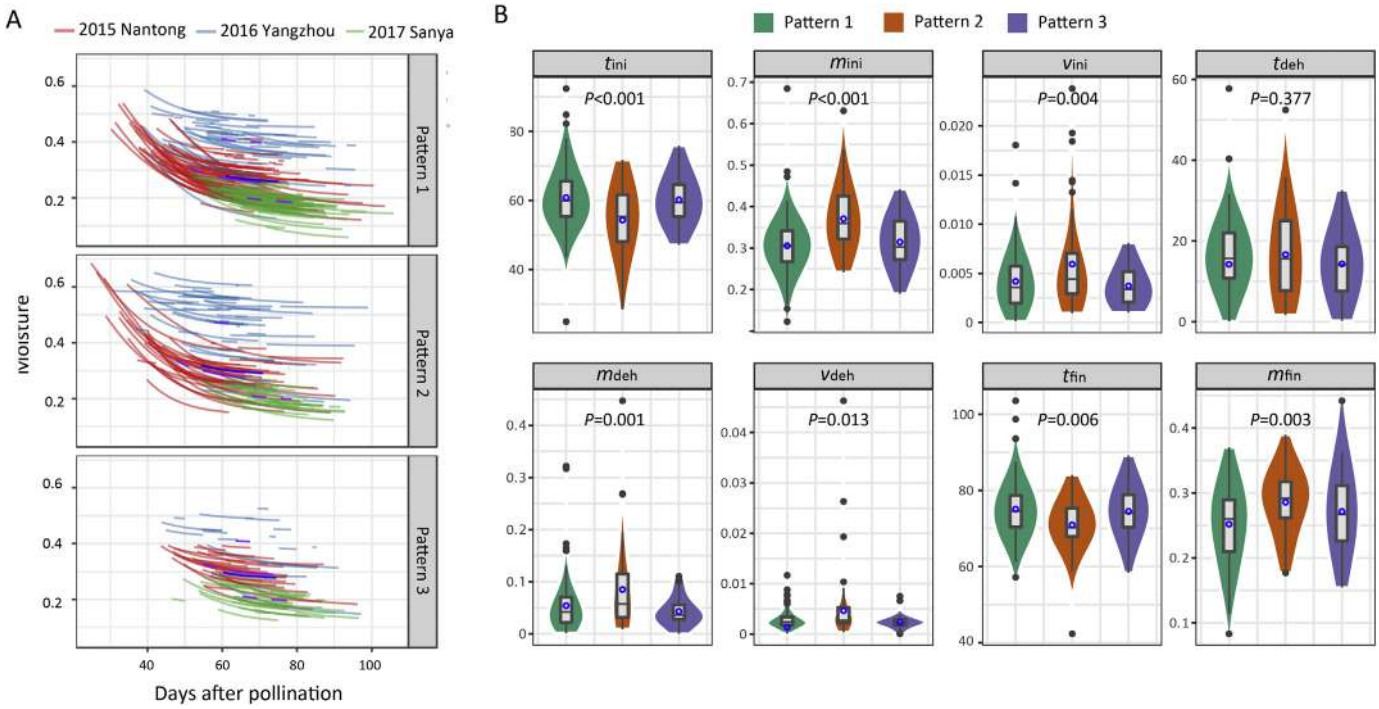

Fig. 7 – Three patterns of the seed dehydration process defined by 12 co-located QTL. A) The dehydration curves of different patterns in three environments, where red, light blue, and green represent dehydration curves for Nantong during 2015, Yangzhou during 2016, and Sanya during 2017, respectively. Purple dashed lines show average dehydration curves in different patterns and environments. Three dark blue solid lines denote the average dehydration curves of the three patterns. B) Distribution of the eight dehydration characteristic parameters in three patterns. All parameters but t_{deh} showed marked differences among the three patterns.

4. Discussion

Seed moisture at harvest is a primary factor affecting maize quality and commercial production. Low seed moisture at harvest can reduce the economic impact of artificial drying and facilitate mechanical harvesting. The dehydration process from physiological maturity to harvesting directly affects final seed moisture. However, because seed dehydration is a continuous dynamic process and corresponding start and end times are difficult to determine accurately, genetic analysis of seed dehydration features is a challenge for researchers. In this study, we used a novel strategy based on the filling curve and the dry weight/fresh weight ratio curve to define the seed dehydration process in maize. We used eight characteristic parameters determining the seed dehydration curve to describe dehydration features. Compared with previous studies, this strategy accurately determined the initial time for dehydration based on the definition of physiological maturity as the point at which the maximum dry weight of the grain is realized [2,10]. In addition, the dehydration duration of each inbred line was estimated rather than taken as a uniform value. The use of eight characteristic parameters allowed research contents associated with seed dehydration to be more varied and not limited to final seed moisture and average dehydration rate.

Understanding the complexity of seed dehydration based on these characteristic parameters would aid in the selection of an optimal breeding strategy. The high heritability of these characteristic parameters suggests the presence of high genetic variation in the segregating population, in which the heritability of final seed moisture and average dehydration rates were similar to those in previous studies [3,27–30]. This result indicates that these characteristic parameters are quantitative “traits” with stable inheritance and can be effectively selected. The correlations between some characteristic parameters were high, suggesting that they may represent similar genetic mechanisms. For the same characteristic parameter, correlations between environments showed low levels, perhaps owing to large environment differences and genotype-environment interaction. Interestingly, the heritabilities of these characteristic parameters showed medium and high levels in this study, suggesting that traits with high heritability might still show low correlations between environments. Considering that heritability is defined as the proportion of genetic variance to phenotypic variance and is affected by many factors, such as experimental design, calculation method, and population type, the heritability may not be directly related to the degree of correlation between environments.

Maize seed dehydration is a complex process that is affected by many external factors [31–33]. Different QTL mapping methods have different detection powers for different traits [34–36]. Therefore, it is necessary to identify QTL associated with dehydration in maize by acquiring dehydration characteristic parameters in multiple environments and

using multiple mapping methods. In this study, we collected seed moisture data in three environments and identified abundant QTL associated with dehydration features using single-trait, multiple-environment, and multiple-trait QTL analysis. A QTL located at 104.1 cM on chromosome 5 was consistent with one QTL identified by Wang [7]. In the same QTL region, *GRMZM5G809727* was identified by genome-wide association analysis (GWAS) [6] as being associated with field grain drying rate. A QTL located at 18.9 cM on chromosome 7 was close to *GRMZM2G029722*, identified as being associated with grain drying rate and predicted to encode cucumber mosaic virus (CMV) 1a interacting protein1 [37]. Three QTL located at 3.9, 68.7, and 145.4 cM on chromosome 8 have also been found in other studies [6,7]. For eight dehydration characteristic parameters, multiple-trait QTL analysis revealed more QTL than other methods, indicating that this method was more powerful because it accounts for the structure of genetic correlations between traits. It can distinguish between pleiotropy and gene linkage as underlying causes of a genetic relationship between traits [38,39]. Twelve co-located QTL associated with dehydration features were determined and the dehydration process was divided into three patterns with significant differences. These co-located QTL are reliable and will be valuable for marker-assisted selection in maize genetic improvement. These results indicate that the research approach used in this study could efficiently identify genetic loci that regulate the dynamic features of seed dehydration.

Supplementary data for this article can be found online at https://doi.org/10.1016/j.cj.2019.06.011.

Declaration of competing interest

The authors declare that they have no known competing financial interests or personal relationships that could have appeared to influence the work reported in this paper.

Acknowledgments

This work was supported by the National Key Research and Development Program of China (2016YFD0100303), the National High Technology Research and Development Program of China (2014AA10A601-5), the Priority Academic Program Development of Jiangsu Higher Education Institutions, the National Natural Science Foundation of China (91535103, 31371632, 31200943), the Natural Science Foundation of Jiangsu Province (BK20150010), the Scientific and Technological Project of Jiangsu Province, China (BE2018325), the Innovative Research Team of Ministry of Agriculture, and the Qing Lan Project of Jiangsu Province.

REFERENCES

[1] A. Cao, R. Santiago, A.J. Ramos, S. Marín, L.M. Reid, A. Butrón, Environmental factors related to fungal infection and fumonisin accumulation during the development and drying of white maize kernels, Int. J. Food Microbiol. 164 (2013) 15–22.

[2] R.H. Shaw, W.E. Loomis, Bases for the prediction of corn yields, Plant Physiol. 25 (1950) 225–244.

[3] B. De Jager, C.Z. Roux, H.C. Kuhn, An evaluation of two collections of South African maize (*Zea mays* L.) germ plasm: 2. The genetic basis of dry-down rate, South Afr. J. Plant Soil 21 (2004) 120–122.

[4] R.G. Sala, F.H. Andrade, E.L. Camadro, J.C. Cerono, Quantitative trait loci for grain moisture at harvest and field grain drying rate in maize (*Zea mays* L.), Theor. Appl. Genet. 112 (2006) 462–471.

[5] J.C. Ho, S.R. McCouch, M.E. Smith, Improvement of hybrid yield by advanced backcross QTL analysis in elite maize, Theor. Appl. Genet. 105 (2002) 440–448.

[6] L.Q. Dai, L. Wu, Q.S. Dong, Z. Zhang, N. Wu, Y. Song, S. Lu, P. W. Wang, Genome-wide association study of field grain drying rate after physiological maturity based on a resequencing approach in elite maize germplasm, Euphytica 213 (2017) 182.

[7] Z.H. Wang, X. Wang, L. Zhang, X.J. Liu, H. Di, T.F. Li, X.C. Jin, QTL underlying field grain drying rate after physiological maturity in maize (*Zea Mays* L.), Euphytica 185 (2012) 521–528.

[8] J.L. Purdy, P.L. Crane, Inheritance of drying rate in “Mature” corn (*Zea mays* L.), Crop Sci. 7 (1967) 294–297.

[9] S.Y. Yin, P.C. Li, Y. Xu, L. Xue, D.R. Hao, J. Liu, T.T. Yang, Z.F. Yang, C.W. Xu, Logistic model-based genetic analysis for kernel filling in a maize RIL population, Euphytica 214 (2018) 86.

[10] I.R. Brooking, Maize ear moisture during grain-filling, and its relation to physiological maturity and grain-drying, Field Crops Res. 23 (1990) 55–68.

[11] G.B. West, J.H. Brown, B.J. Enquist, A general model for ontogenetic growth, Nature 413 (2001) 628–631.

[12] G.A. Milliken, D.M. Bates, D.G. Watts, Non-linear regression analysis and its applications, Technometrics 32 (1988) 219–220.

[13] S.J. Knapp, W.W. Stroup, W.M. Ross, Exact confidence intervals for heritability on a progeny mean basis, Crop Sci. 25 (1985) 192–194.

[14] L.I. Lin, A concordance correlation coefficient to evaluate reproducibility, Biometrics 45 (1989) 255–268.

[15] F. de Mendiburu, Agricolae: statistical procedures for agricultural research, R Packag, Version 1 (2014) 1–8.

[16] M.W. Ganal, G. Durstewitz, A. Polley, A. Bérard, E.S. Buckler, A. Charcosset, J.D. Clarke, E.M. Graner, M. Hansen, J. Joets, M.C. le Paslier, M.D. McMullen, P. Montalent, M. Rose, C.C. Schön, Q. Sun, H. Walter, O.C. Martin, M. Falque, A large maize (*Zea mays* L.) SNP genotyping array: development and germplasm genotyping, and genetic mapping to compare with the B73 reference genome, PLoS One 6 (2011), e28334.

[17] X.H. Huang, Q. Feng, Q. Qian, Q. Zhao, L. Wang, A. Wang, J.P. Guan, D.L. Fan, Q.J. Weng, T. Huang, G.J. Dong, T. Sang, B. Han, High-throughput genotyping by whole-genome resequencing, Genome Res. 19 (2009) 1068–1076.

[18] K.W. Broman, H. Wu, S. Sen, G.A. Churchill, R/qtl: QTL mapping in experimental crosses, Bioinformatics 19 (2003) 889–890.

[19] D.D. Kosambi, The estimation of map distances from recombinantion values, Ann. Hum. Genet. 12 (1943) 172–175.

[20] S.S. Li, J.K. Wang, L.Y. Zhang, Inclusive composite interval mapping of QTL by environment interactions in biparental populations, PLoS One 10 (2015), e0132414.

[21] J.K. Wang, Inclusive composite interval mapping of quantitative trait genes, Acta Agron. Sin. 35 (2009) 239–245(in Chinese with English abstract).

[22] L. Meng, H.H. Li, L.Y. Zhang, J.K. Wang, QTL IciMapping: integrated software for genetic linkage map construction and quantitative trait locus mapping in biparental populations, Crop J. 3 (2015) 269–283.

[23] C.J. Jiang, Z.B. Zeng, Multiple trait analysis of genetic mapping for quantitative trait loci, Genetics 140 (1995) 1111–1127.
[24] C.H. Kao, Z.B. Zeng, R.D. Teasdale, Multiple interval mapping for quantitative trait loci, Genetics 152 (1999) 1203–1216.
[25] E.C. Neto, M.P. Keller, A.F. Broman, A.D. Attie, R.C. Jansen, K. W. Broman, B.S. Yandell, Quantile-based permutation thresholds for quantitative trait loci hotspots, Genetics 191 (2012) 1355–1365.
[26] E.C. Neto, A.T. Broman, M.P. Keller, A.D. Attie, B. Zhang, J. Zhu, B.S. Yandell, Modeling causality for pairs of phenotypes in system genetics, Genetics 193 (2013) 1003–1013.
[27] M.S. Kang, S. Zhang, Narrow-sense heritability for and relationship between seed imbibition and grain moisture loss rate in maize, J. New Seeds 3 (2001) 1–16.
[28] R. Magari, M.S. Kang, Y. Zhang, Genotype by environment interaction for ear moisture loss rate in corn, Crop Sci. 37 (1997) 774–779.
[29] H.G. Nass, P.L. Crane, Effect of endosperm mutants on drying rate in corn (*Zea mays* L.), Crop Sci. 10 (1970) 141–144.
[30] D.F. Austin, M. Lee, L.R. Veldboom, A.R. Hallauer, et al., Crop Sci. 40 (2000) 30–39.
[31] Z. Ristic, G. Williams, G. Yang, B. Martin, S. Fullerton, Dehydration, damage to cellular membranes, and heat-shock proteins in maize hybrids from different climates, J. Plant Physiol. 149 (1996) 424–432.
[32] P.M. Sweeney, S.K. St. Martin, C.P. Clucas, Indirect inbred selection to reduce grain moisture in maize hybrids, Crop Sci. 34 (1994) 391–396.
[33] Z. Ristic, M.A. Jenks, Leaf cuticle and water loss in maize lines differing in dehydration avoidance, J. Plant Physiol. 159 (2002) 645–651.
[34] K. MacMillan, K. Emrich, H.P. Piepho, C.E. Mullins, A.H. Price, Assessing the importance of genotype × environment interaction for root traits in rice using a mapping population II: conventional QTL analysis, Theor. Appl. Genet. 113 (2006) 953–964.
[35] B. Yu, K. Boyle, W. Zhang, S.J. Robinson, E. Higgins, L. Ehman, J.A. Relf-Eckstein, G. Rakow, I.A.P. Parkin, A.G. Sharpe, P.R. Fobert, Multi-trait and multi-environment QTL analysis reveals the impact of seed colour on seed composition traits in Brassica napus, Mol. Breed. 36 (2016) 111.
[36] N.A. Alimi, M.C.A.M. Bink, J.A. Dieleman, J.J. Magan, A.M. Wubs, A. Palloix, F.A. van Eeuwijk, Multi-trait and multi-environment QTL analyses of yield and a set of physiological traits in pepper, Theor. Appl. Genet. 126 (2013) 2597–2625.
[37] M.J. Kim, S.U. Huh, B.K. Ham, K.H. Paek, A novel methyltransferase methylates *Cucumber mosaic virus* 1a protein and promotes systemic spread, J. Virol. 82 (2008) 4823–4833.
[38] L.D. Costa, E. Silva, S. Wang, Z. Zeng, Multiple trait multiple interval mapping of quantitative trait loci from inbred line crosses, BMC Genet. 13 (2012) 67.
[39] M.V. Sukhwinder-Singh, J. Hernandez, P.K. Crossa, N.S. Singh, K. Bains, I. Sharma Singh, Multi-trait and multi-environment QTL analyses for resistance to wheat diseases, PLoS One 7 (2012), e38008.